

TRI-PP--90-16

2 pages

Invited talk presented at the International Workshop,
Rare Decays of Light Mesons, Gif-sur-Yvette, March 29-30

TRI-PP-90-16
Mar 1990

SEARCH FOR THE RARE DECAY $K^+ \rightarrow \pi^+ \nu \bar{\nu}$

presented by J-M Poutissou

Collaboration Brookhaven-Los Alamos-Princeton-TRIUMF*

A description of the search for the rare decay $K^+ \rightarrow \pi^+ \nu \bar{\nu}$ at Brookhaven National Laboratory is presented. Results from the 1988 first run are discussed and expectations for the 1989 data set will be outlined. Other branches have been searched for using the same detector, and preliminary results are given for $K^+ \rightarrow \pi^+ \mu^- \mu^+$ and $K^+ \rightarrow \pi^+ \gamma \gamma$.

*M. Atiya, I-H Chiang, J.S Frank, J.S. Haggerty, M.M. Ito, T.F. Kycia, K.K. Li, L.S. Littenberg, A. Sambamurti, A. Stevens, R.C. Strand (Brookhaven National Laboratory), W.C. Louis (Los Alamos National Laboratory), D. Akerib, D. Marlow, P.D. Meyers, M.A. Selen, F.C. Shoemaker, A.J.S. Smith (Princeton University), G. Azuelos, E. Blackmore, D. Bryman, L. Felawka, P. Kitching, Y. Kuno, J.A. Macdonald, P. Padley, J-M Poutissou, R. Poutissou, J. Roy, R. Soluk, A. Turcot (TRIUMF).

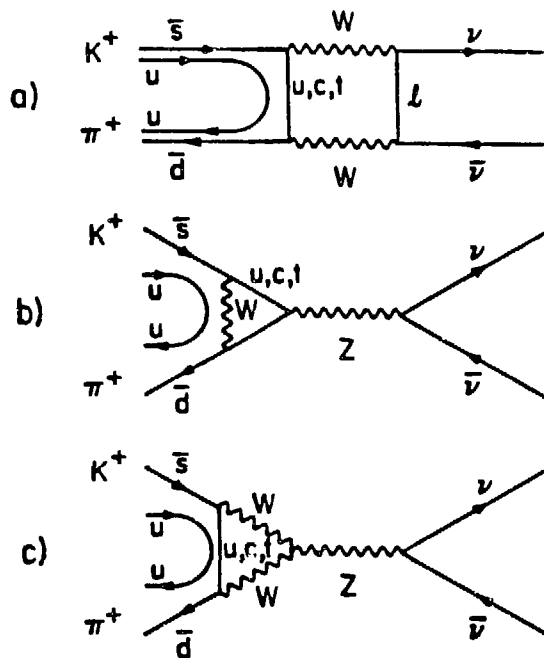


Fig. 1. Second-order diagrams for $K^+ \rightarrow \pi^+ \nu \bar{\nu}$.

Kaon decays have been very fruitful in establishing major ingredients of the standard model. They will continue to do so with the availability of better beams and higher intensities. After 20 years of very active research, some of the crucial tests of the standard model are still performed in the K system (CP violation, mixing, renormalization of the theory, ...).

The rare decay $K^+ \rightarrow \pi^+ \nu \bar{\nu}$ offers a unique opportunity to test second-order weak processes because the neutral leptons in the final state do not allow large, long-distance contributions. $K^+ \rightarrow \pi^+ \nu \bar{\nu}$ is a flavour-changing neutral current process which is forbidden in first order by the Glashow-Iliopoulos-Maiani mechanism (GIM) and occurs through higher-order weak diagrams such as described in fig. 1. A similar situation exists for the decay $K_L^0 \rightarrow \mu^+ \mu^-$ except for the fact that electromagnetic effects in the final state dominate the rate, making the estimate of the weak contribution unreliable.

The six-quark standard model prediction for the branching ratio for $K \rightarrow \pi \nu \bar{\nu}$ is quite constrained by our knowledge of the Kobayashi-Maskawa mixing matrix (K-M matrix),²⁾ and it lies in the range $(1-8) \times 10^{-10}$ which is accessible to our experiment E787 mounted at the Alternating Gradient Synchrotron (AGS) at the Brookhaven National Laboratory.

More specifically the branching ratio per neutrino flavour is given by

$$B(K^+ \rightarrow \pi^+ \nu \bar{\nu}) = \frac{0.61 \times 10^{-6}}{|V_{us}|^2} \left| \sum_{j=c,t} V_{js}^* V_{jd} D(x_j) \right|^2,$$

where $x_j = (m_j^2)/(m_w^2)$, m_j and m_w being the masses of the quarks and of the intermediate vector boson, respectively. V_{ij} are the elements of the K-M matrix. Both c and t quark

en National
stitutions for
the same

Littenberg,
Los Alamos
ker, A.J.S.
Kitching,
A. Turcot

contributions are important, and consequently the branching ratio is sensitive to the mass of the top quark. The main uncertainties come from our knowledge of the K-M matrix elements. The observation of a signal in the range $(1-8) \times 10^{10}$ would place severe constraints on the top quark mass and/or the K-M matrix. An observation of a rate larger than 8×10^{10} would be interpreted as evidence for new physics not included in the standard model, such as extra lepton or quark families, new light weakly interacting particles predicted in extensions of the standard model: supersymmetric particles, majoron, axion, familon.

Other decay modes can also be searched for by the same detector, and the first data runs have led to new upper limits for $K^+ \rightarrow \pi^+ \mu^+ \mu^-$, $K^+ \rightarrow \pi^+ \gamma \gamma$ (preliminary), $\pi^0 \rightarrow \nu \bar{\nu}$ (preliminary), etc.

The signature for $K \rightarrow \pi \nu \bar{\nu}$ is a single charged pion track. The more prolific decays $K \rightarrow \pi^+ \pi^0$ ($K_{\pi 2}$), $K^+ \rightarrow \mu^+ \nu_\mu$ have to be eliminated. By measuring the momentum, the energy and range of the charged track, π^+ can be identified in the part of phase space above the $K_{\pi 2}$ branch. Furthermore, we identify a positive pion by requiring that the decay muon (4.1 MeV) be seen as well as the positron from the decayed muon. To reach the level of sensitivity of 2×10^{-10} , a large solid angle spectrometer has been developed and is schematically represented in fig. 2.

A cylindrically symmetric detector has been built and is located inside a 3 m diameter solenoidal magnet which produces a 1 T field with very good uniformity (<1%) over the volume of the tracking drift chamber. 775 MeV/c kaons from the LESB1 beam line are brought to rest in a segmented scintillating fibre target at a rate of 300 K/spill (a spill lasts 1.8 s and occurs every ~ 3 s). Pions in the beam (ratio $\pi : K = 2.5 : 1$) are identified by a lucite radiator Čerenkov counter as well as in highly segmented beam counters. The stopping target is made of 379 triangular clusters of six 2 mm diameter scintillating fibres³⁾ read out by a 1 cm diameter phototube. Energy loss and time information are used. The target fibres are 3 m long and provide for some photon rejections in the beam region. The active part of the target is defined by 6 scintillating counters (20 cm long) enclosing the fibre assembly (1 counters). The charged particle momentum is then analysed in a cylindrical drift chamber⁴⁾ made of 5 superlayers (2 of them stereo) of six sense wire cells. The pions then enter a scintillator range stack comprising 12 layers of 2 m long scintillator slabs segmented azimuthally in 24 sectors. Each slab is viewed at each end by a 5 cm diameter phototube, providing a good measurement of the energy deposited, a crude location of the stopping region where a search is conducted for the ensuing muon and positron decay products. To refine the estimate of the range of the pion, a set of 2 proportional chambers is embedded in each sector of the range stack to provide axial position information.

The search for the decay sequence $\pi \mu e$ in the stopping counter is made by using 500 MHz transient digitizers (TDs)⁵⁾ allowing an 8-bit pulse height measurement every 2 ns. The whole range stack is instrumented with such devices, with a multiplexing level of 4. This allows examination of the detector for $\pm 5 \mu\text{s}$ around any candidate trigger. The active pion detector

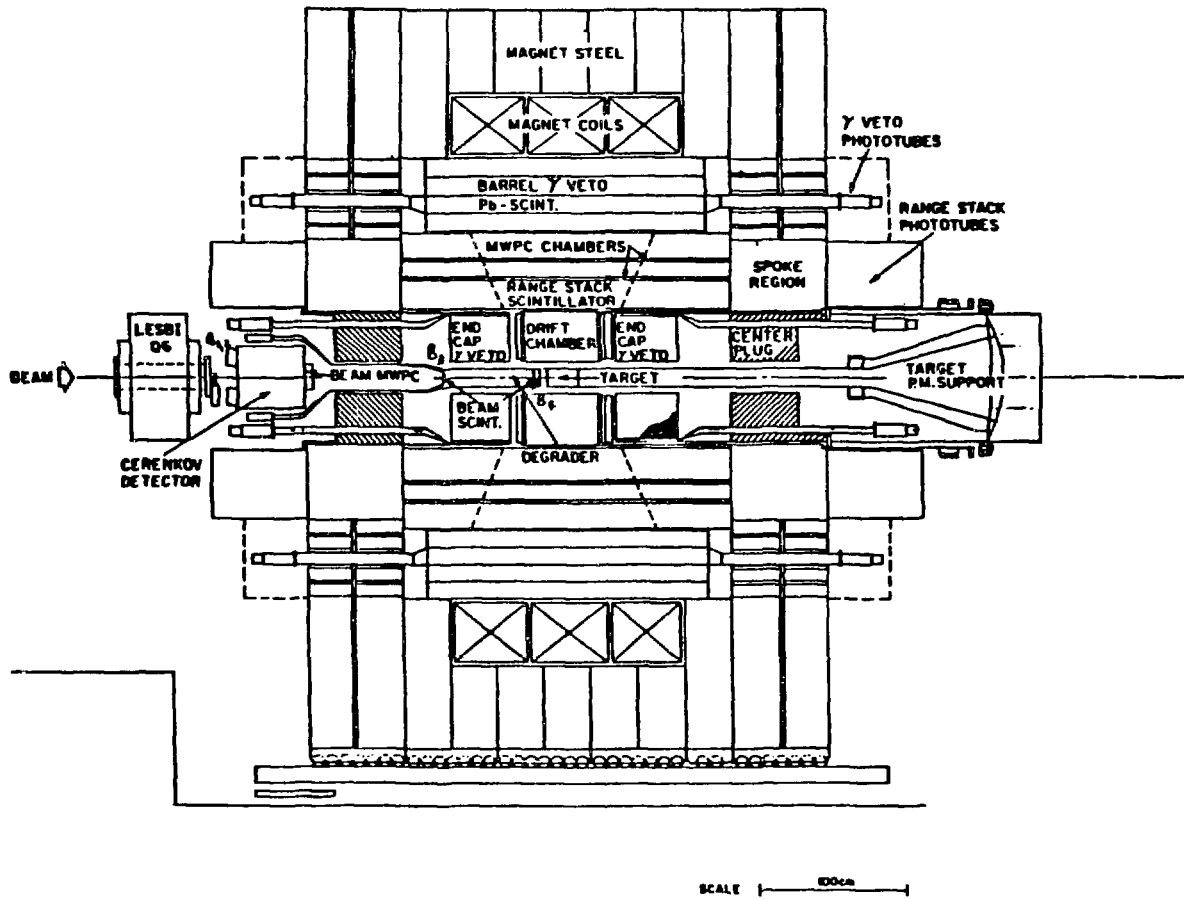


Fig. 2. Schematic side view of the E787 detector.

L0 KP2
L1 KP2
L2 NOTD

SCALE 1:15.0

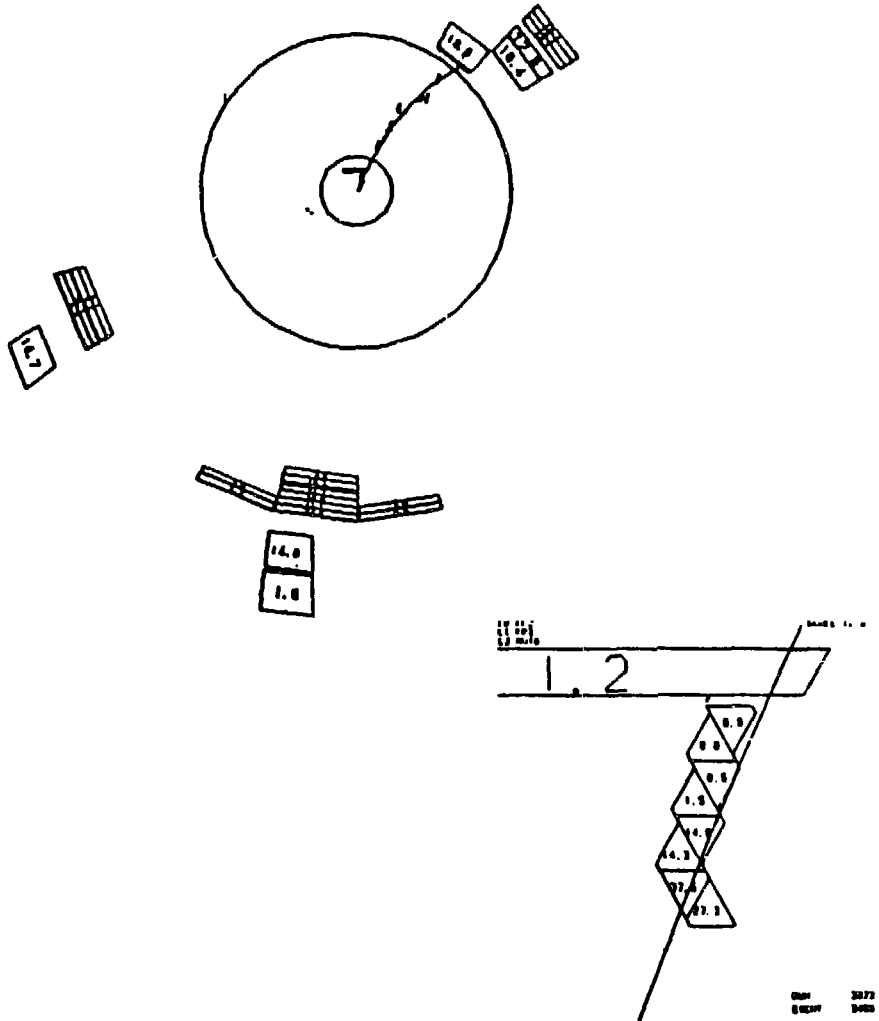


Fig. 3. Typical K_{x2} event, showing elements of detector. Bottom right-hand corner shows enlargement of the target region.

is finally surrounded by a lead-scintillator sandwich photon veto with a coverage of close to 4π sr solid angle. The inefficiency for detecting photons associated with $K^+ \rightarrow \pi^+ \pi^0$ is of order 1×10^{-6} and is dominated by photonuclear products escaping detection.

The main difficulty of the experiment resides in dealing with very high rate of events. A three-level trigger decision scheme is used to select potential candidates at a rate of 30 events per spill. In the off-line analysis, π^+ tracks are identified in the target, the drift chamber and the range stack. The rms resolution for energy, momentum and range measurement was 2.9%, 2.6%, and 4.2%, respectively, in our first data sample.

The highly segmented target is a very powerful device to examine possible background or other tracks associated with other branches like $K^+ \rightarrow \pi^+ \mu^+ \mu^-$, $K^+ \rightarrow \pi^+ e^+ e^- \dots$. Its timing information allows us to search for decays as soon as 2 ns after a kaon has stopped. An example of a $K_{\pi 2}$ event is shown in fig. 3.

An engineering run in 1988 led to a sample of 1.24×10^{10} stopped kaons over a two-week period. This sample has now been fully analysed and results are available or in preliminary form. For $K^+ \rightarrow \pi^+ \nu \bar{\nu}$ the net acceptance (after all analysis cuts) was 0.55% where the most significant losses are the phase space region above the $K_{\pi 2}$ peak (17%), the solid angle of the tracking detector (47%) and the $\pi \rightarrow \mu \rightarrow e$ tagging (41%). No events were observed in the signal region (fig. 4) allowing us to quote an upper limit (90% C.L.) for the branching ratio of $< 3.4 \times 10^{-8}$,⁶⁾ a factor of 4 improvement over the previous limit obtained at KEK by Asano *et al.*⁷⁾ A similar analysis for the branch $K \rightarrow \pi X^0$ ($M_{X^0} = 0$) leads to upper limits of $< 6.4 \times 10^{-9}$. Limits can also be obtained for $M_{X^0} > 0$ but depend on the decay products and the lifetime of particle X^0 .

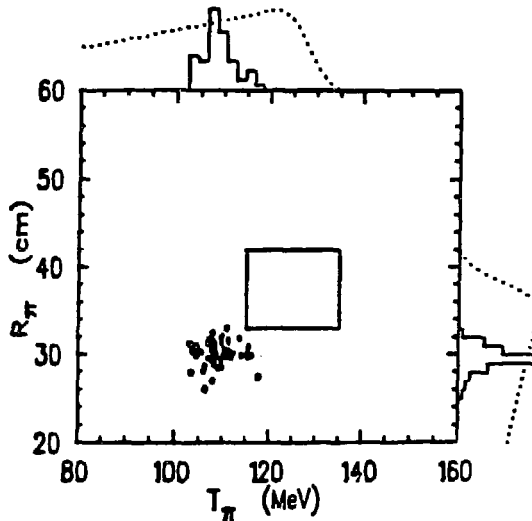


Fig. 4. Range versus energy for events satisfying the selection criteria and having measured momenta $205 < P_\pi < 243$ MeV/c. The rectangular box indicates the search region for $K^+ \rightarrow \pi^+ \nu \bar{\nu}$ and $K^+ \rightarrow \pi^+ X^0 (M_{X^0} = 0)$.

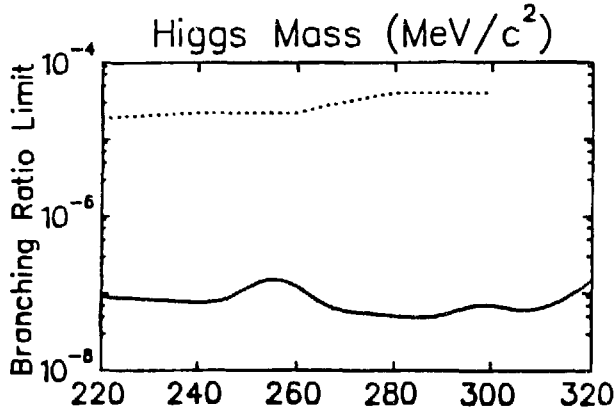


Fig. 5. The 90% confidence level upper limits of the branching ratio for the decay $K^+ \rightarrow \pi^+ H$, $H \rightarrow \mu^+ \mu^-$, as a function of M_H (solid line). Also shown (dashed line) is the result of an inclusive search for $K^+ \rightarrow \pi^+ X^0$.

The detector just described is also capable of other physics studies. As part of our standard mix of triggers, we searched for the branches $K^+ \rightarrow \pi^+ \mu^+ \mu^-$ and $K^+ \rightarrow \pi^+ \gamma \gamma$. For $K^+ \rightarrow \pi^+ \mu^+ \mu^-$, events for which two charged tracks reached the first 3 layers of the range stack were examined. Two tracks of positive curvature, one of negative curvature were demanded in the drift chamber and/or in the target. In an exposure of 9.6×10^9 stopped kaons, 3 events survived the analysis which were consistent with $K^+ \rightarrow \pi^+ \mu^+ \mu^-$. Interpreted as an upper limit, the branching ratio for this branch has to be $< 2.3 \times 10^{-7}$.⁸⁾

The same final state can be reached via

$$K^+ \rightarrow \pi^+ H^0 \\ \quad \quad \quad \hookrightarrow \mu^+ \mu^- ,$$

where H^0 is a light Higgs boson. In the mass region $2m_\mu < M_{H^0} < (m_K - m_\pi)$, H^0 decays mainly via $\mu^+ \mu^-$ with a lifetime $< 10^{-14}$. In fig. 5 we show the limits improvements realised by this search in the interval 220–320 MeV.

By demanding a coincidence between a charged track and two photons a search of the decay branch $K \rightarrow \pi \gamma \gamma$ was conducted in a region of phase space excluding K_{s2} . The same signature arises from processes like $K^+ \rightarrow \pi^+ X^0$; $X^0 \rightarrow \gamma \gamma$, where X^0 is a massive short-lived scalar particle or a light Higgs boson decaying via $H^0 \rightarrow \gamma \gamma$. In this case we are mainly sensitive to masses from 0 to 100 MeV/c². Predictions for the branching ratio $K^+ \rightarrow \pi^+ \gamma \gamma$ exist within a framework of chiral perturbation theory in the range 10^{-6} – 10^{-7} .^{9,10)} The 4 π photon veto described above was used as an electromagnetic calorimeter with resolution $\sigma_E/E = 8/\sqrt{E}\%$ (E in GeV), and minimum energy and range cuts were imposed on the π^+ to reject $K^+ \rightarrow \pi^+ \pi^0$ events.

Figure 6 shows the reconstructed $\gamma \gamma$ masses for all good $\pi \gamma \gamma$ events. There are no events between 0 and 99 MeV/c² for the region with a confidence level $> 95\%$. The large model

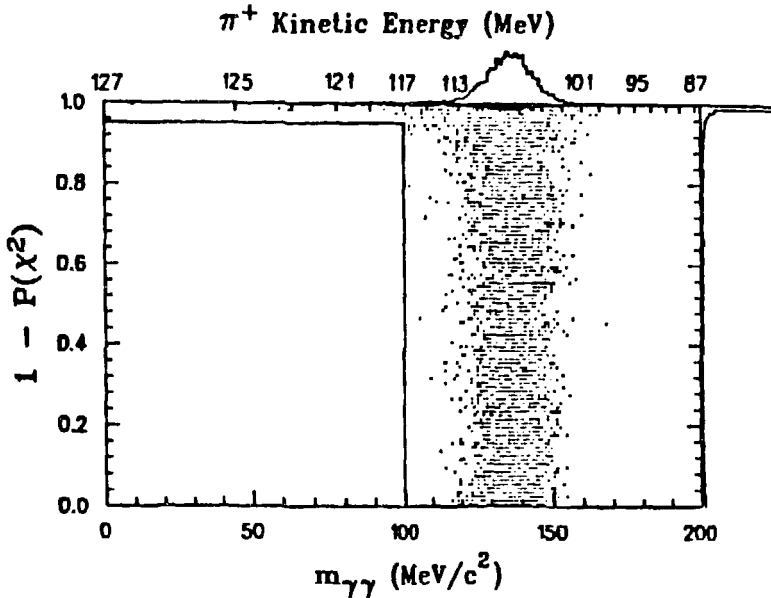


Fig. 6. Scatter plot of $M_{\gamma\gamma}$ vs. confidence level for the final sample of $K^+ \rightarrow \pi^+\gamma\gamma$ events. The box represents the region of 95% confidence level used to extract the branching ratio.

dependence of the acceptance for $K^+ \rightarrow \pi^+\gamma\gamma$ events does not allow quoting an absolute branching ratio limit. Assuming a pure phase space distribution (unit matrix element) one can quote a preliminary upper limit of 1.0×10^{-6} , a factor 8 improvement over previous studies. But chiral perturbation theories generate distributions which are very different. Using ref. 10, for example, would reduce the upper limit to 1.5×10^{-4} . Other decay modes can be searched for and, for example, an upper limit of $< 10^{-6}$ has been preliminarily established for the decay $\pi^0 \rightarrow \nu\bar{\nu}$.

Table I presents a summary of our results from the analysis of our first data set in 1988. Since then we have accumulated about 10 times the amount of data, which are still under analysis. The experiment is currently taking data at a slightly faster rate (300 K stopped per spill compared to 150 K for the data of 1988).

Table I. Summary

Decay	Limit	Status
$K \rightarrow \pi^+\nu\bar{\nu}$	$< 3.4 \times 10^{-8}$	published (ref. 6)
$\pi^0 \rightarrow \nu\bar{\nu}$	$< 1 \times 10^{-6}$	preliminary
$K \rightarrow \pi^+\gamma\gamma$	$< 1 \times 10^{-6}$	preliminary
$K \rightarrow \pi^+X, X \rightarrow \gamma\gamma$	$< (1-2) \times 10^{-7}$	preliminary
$K \rightarrow \pi^+H, H \rightarrow \mu\mu$	$< 1.5 \times 10^{-7}$	published (ref. 8)
$K \rightarrow \pi^+\mu^+\mu^-$	$< 2.3 \times 10^{-7}$	published (ref. 8)
$K \rightarrow \mu^+\nu\mu^+\mu^-$	$< 4.1 \times 10^{-7}$	published (ref. 8)

To reach our goal of 2×10^{-10} sensitivity, we must increase our stopping rate by another factor 3, which we hope to achieve with the commissioning of an improved beam line as proposed by Doornbos *et al.*¹¹⁾ Concurrently, improvements are being considered for the detector; brighter scintillating fibres are now available with square cross section allowing for less non-active material in the target. A new axial vertex chamber would allow an improvement in the momentum resolution. Totally active fast scintillators like CsI (pure) could be used to partially replace the lead-scintillator sandwich increasing the visible energy by 50%.

We believe that the standard model prediction can be tested within the next few years. A detailed study of the pion spectrum for $K^+ \rightarrow \pi^+ \nu \bar{\nu}$ must await the higher fluxes at the KAON factory and will represent the challenge for the next generation of experiments.

References

1. T. Inami and C.S. Lim, *Prog. Theor. Phys.* **65**, 297 (1981);
J. Ellis, J.S. Hagelin and S. Rudaz, *Phys. Lett. B* **192**, 201 (1987);
J. Ellis, J.S. Hagelin, S. Rudaz and D.D. Wu, *Nucl. Phys.* **B304**, 205 (1988);
C.O. Dib, I. Duneitz and F.J. Gilman, SLAC preprint SLAC.PUB-4840 (1989).
2. M. Kobayashi and T. Maskawa, *Prog. Theor. Phys.* **49**, 652 (1973).
3. J.S. Frank and R.S. Strand, *Proceedings of the Workshop on Scintillating Fiber Development for the SSC, Fermi National Accelerator Laboratory, November 14-16, 1988.*
4. J.V. Cresswell, S. Ahmad, E.W. Blackmore, D.A. Bryman, N. Khan, Y. Kuno and T. Numao, *Cylindrical drift chamber for the measurement $K \rightarrow \pi \nu \bar{\nu}$ decay*, *IEEE Trans. Nucl. Sci.* **35**, 460 (1988).
5. M.S. Atiya *et al.*, *Nucl. Instrum. Methods* **A279**, 180 (1989).
6. M.S. Atiya *et al.*, *Phys. Rev. Lett.* **64**, 21 (1990).
7. Y. Asano *et al.*, *Phys. Lett.* **107B**, 159 (1981).
8. M.S. Atiya *et al.*, *Phys. Rev. Lett.* **63**, 2177 (1989).
9. G. Ecker, A. Pich and E. de Rafael, UWThPh-1989-65, FTUV/89-44, CPT-89/P.E 2325 (1989).
10. H-Y. Cheng, BNL preprint 43466 (1989).
11. J. Doornbos, TRIUMF private communication.